Vacuum 83 (2009) S275–S279

Contents lists available at ScienceDirect

Vacuum

journal homepage: www.elsevier.com/locate/vacuum

Electrical properties of nanostructures $(CoFeZr)_x + (Al_2O_3)_{1-x}$ with use of alternating current

P. Żukowski [a,*], T. Kołtunowicz [a], J. Partyka [a], Yu. A. Fedotova [b], A.V. Larkin [c]

[a] Lublin University of Technology, 38a Nadbystrzycka St., 20-618 Lublin, Poland
[b] National Center of Particles and High Energy Physics of BSU, 153 Bogdanovich St., 220040 Minsk, Belarus
[c] Belarusian State University, 4 Nezavisimosti Ave., 220050 Minsk, Belarus

ARTICLE INFO

Article history:
Received 16 June 2008
Received in revised form
29 January 2009
Accepted 30 January 2009

Keywords:
Ion-beam sputtering
Granular nanocomposites
Percolation
AC conductance

ABSTRACT

$CoFeZr–Al_2O_3$ nanocomposite films of 3–5 μm thickness, containing metallic alloy nanoparticles embedded into the dielectric alumina matrix, have been deposited on a glass ceramic substrate using magnetron sputtering of composite target in Ar gas ambient. Measurements of AC conductance and lagging have been performed within the frequency range of 50 Hz–1 MHz at the temperatures from 79 K to 373 K in the initial (as-deposited) samples as well as directly after their isochronous (15 min) annealings within the temperature range from 398 K to 648 K with 25 K step.

The observed variations of real part AC electrical conductivity with temperature and frequency $\sigma_{real}(T, f)$ in the as-deposited films display transition from dielectric to metallic behaviour when crossing the percolation threshold x_C in the studied nanocomposites. After annealing of the samples below the x_C the $\sigma_{real}(T, f)$ progress follows the hopping law of electron conductivity with sigmoidal frequency dependence. The samples being far beyond the percolation threshold revealed transition from metallic to activational $\sigma_{real}(T)$ law after high-temperature annealing attributed to the internal oxidation of metallic nanoparticle by excess of oxygen presented in the as-deposited samples.

1. Introduction

Among nanostructured materials granular nanocomposites FeCo-based ferro-magnetic alloy – amorphous dielectric matrix rank a special place. Though looking homogeneous on the macroscopic scale, such binary composite nanostructures are disordered and inhomogeneous in nanoscale. Depending on the metallic phase concentration x, the electrical properties of such mixtures can be varied between those of the matrix and those of the filler. In the typical binary composite materials a critical concentration, percolation threshold x_C [1], is reached when a continuous conducting cluster of filler (metallic phase) particles is formed through the sample.

Important applications of these systems are conductive adhesives, protection layers against electromagnetic radiation and novel electronic and magnetoelectronic devices [2]. Note that granular metal-dielectric nanocomposites (MDNC) with randomly distributed metallic nanoparticles in the dielectric matrix, show extremal characteristics (including the highest values of tunneling magnetoresistance (TMR) effect) just at approaching the x_C [1] when metallic nanoparticles only begin to form continuous current conducting metallic net. This makes MDNCs with the percolative configuration very attractive for the manufacturing of magneto-sensors working in high-frequency regimes.

As follows changing the position of the x_C gives the possibility to tune the composite properties. The controllable thermal subjections after the composite synthesis can be one of the important methods for varying the x_C position and therefore changing structural and electric properties of the MDNC materials.

The goal of this paper is to investigate the influence of short isochronous annealings on AC conductivity of the composite films $(FeCoZr)_x–(Al_2O_3)_{100-x}$ deposited in pure argon ambient.

2. Experimental

The $(Co_{45}Fe_{45}Zr_{10})_x(Al_2O_3)_{100-x}$ films of 3–5 μm thicknesses were prepared by ion-beam sputtering in a chamber evacuated with pure argon at a pressure of 8.0×10^{-2} Pa. A special construction of compound target allowed getting the film with a wide region of metal-to-dielectric ratios x ($31 \le x \le 64$ at.%) on the class ceramic substrate in one deposition procedure [3].

Measurements of AC conductance σ and lagging $tg\delta$ have been performed within the frequency range of $f = 50$ Hz ÷ 1 MHz at the temperatures T from 79 K to 373 K for the samples in the initial

* Corresponding author. Fax: +48 81 538 4575.
E-mail address: pawel@elektron.pol.lublin.pl (P. Żukowski).

0042-207X/$ – see front matter © 2009 Elsevier Ltd. All rights reserved.
doi:10.1016/j.vacuum.2009.01.081

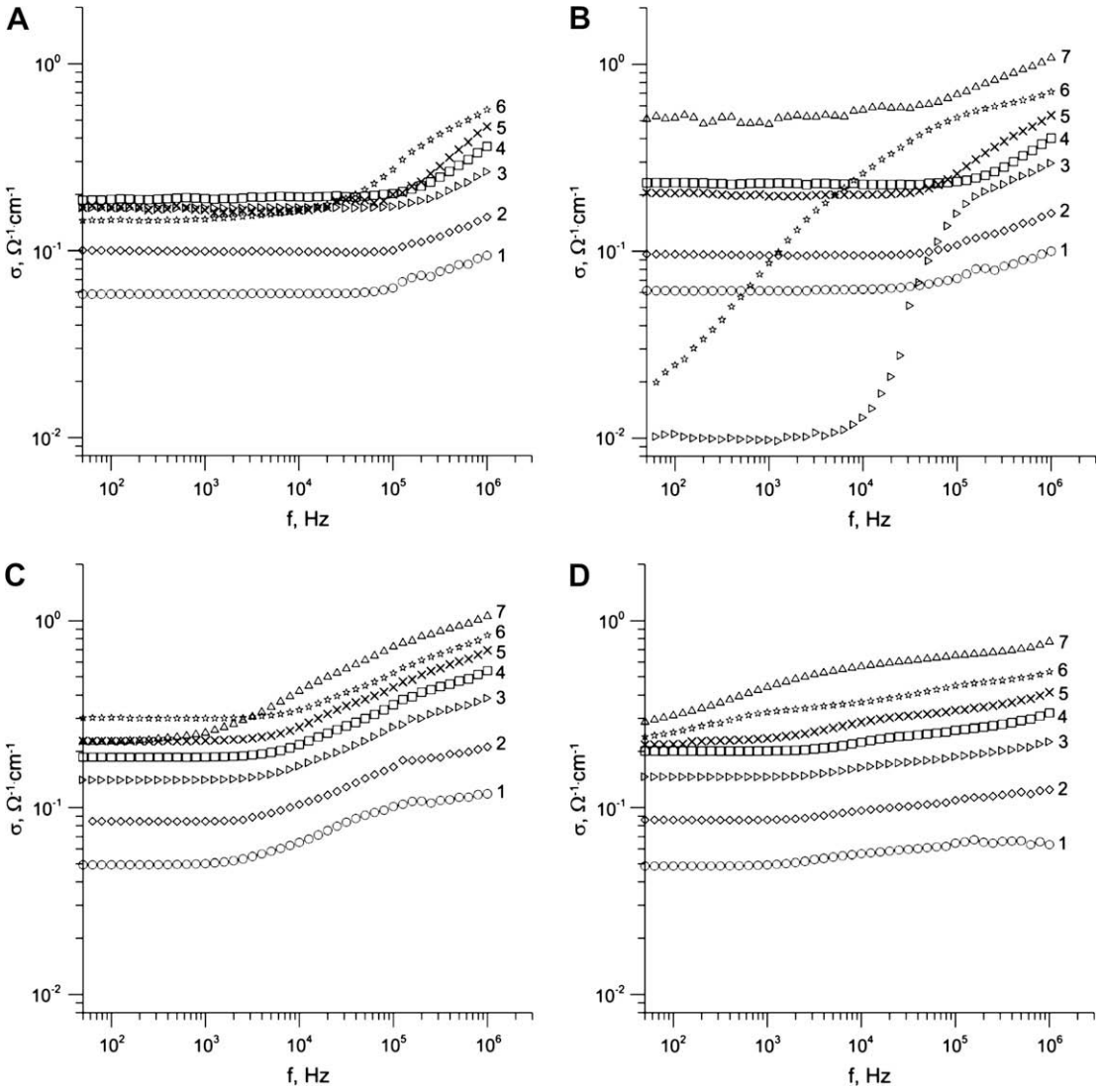

Fig. 1. $\sigma_{real}(T, f)$ dependences for the sample with $x \approx 31$ at.% at different isochronous annealing temperatures T_{ann}: A – as-deposited; B – $T_{ann} = 398$ K; C – 548 K; D – 648 K; 1 – $T = 79$ K; 2 – 113 K, 3 – 158 K, 4 – 203 K, 5 – 248 K, 6 – 288 K and 7 – 353 K.

(as-deposited) state as well as directly after their isochronous (15 min) annealing in a tubular furnace within the temperature range from 398 K to 673 K with the 25 K step.

Depth distributions of the elements in the composites were determined by Backscattering Spectrometry with the ion beam of 2.9 MeV $^4He^+$ obtained from a 5 MeV Van der Graaff accelerator.

Preliminary investigation of the Mössbauer spectra, magnetization, magneto-resistance and DC/AC conductance of the studied MDNCs have revealed that their magnetic state and carrier transport properties were strongly dependent on the metal-to-dielectric ratios x [4–7]. In particular, before the percolation threshold ($x < x_C \approx 45$–47 at.%) nanocomposites showed superparamagnetic state whereas beyond the x_C they were in the ferro-magnetic state. Moreover, it was proved that the mechanism of electron transport in the studied films was changed from hopping by localized states in the dielectric Al_2O_3 matrix to metallic regime when crossing the x_C.

3. Results and discussion

The results of temperature-frequency dependences for real part of AC conductivity $\sigma_{real}(T, f)$ before and after some stages of 15 min annealings are shown in Figs. 1–3 for the samples of three characteristic compositions: with x values of ≈ 31 at.% (far below the x_C), ≈ 42 at.% (near the x_C) and ≈ 64 at.% (far beyond the x_C). The comparison of $\sigma_{real}(T, f)$ dependences, presented in these figures, shows that their behaviour for the films studied is strongly changed when crossing x_C for both the as-deposited films and the samples subjected to isochronous annealing.

As follows from our experiments (see, Fig. 1a), in the composition region of $31 < x < 40$ at.% curves $\sigma_{real}(T)$ for as-deposited samples are not dependent on frequency at $f < 100$ kHz and characterized by positive temperature coefficient of conductivity ($d\sigma/dT$) at $T < 290$ K which is changed into $(d\sigma/dT) > 0$ with their smaller absolute magnitudes at $T > 290$ K. At $f > 100$ kHz we can observe in the as-deposited samples appearance of $\sigma_{real}(f)$ dependences at all measurement temperatures and a monotonous increase of σ_{real} with T that confirms the predominance of activational character of conductivity (with hopping of electrons at the localized states in the alumina matrix [7]).

After annealings (see, Fig. 1b–d) σ_{real} for most temperatures T begins to depend on frequency at $f < 50$ kHz remaining as before invariable at lower f. Moreover, for the films with $x < 40$ at.% some

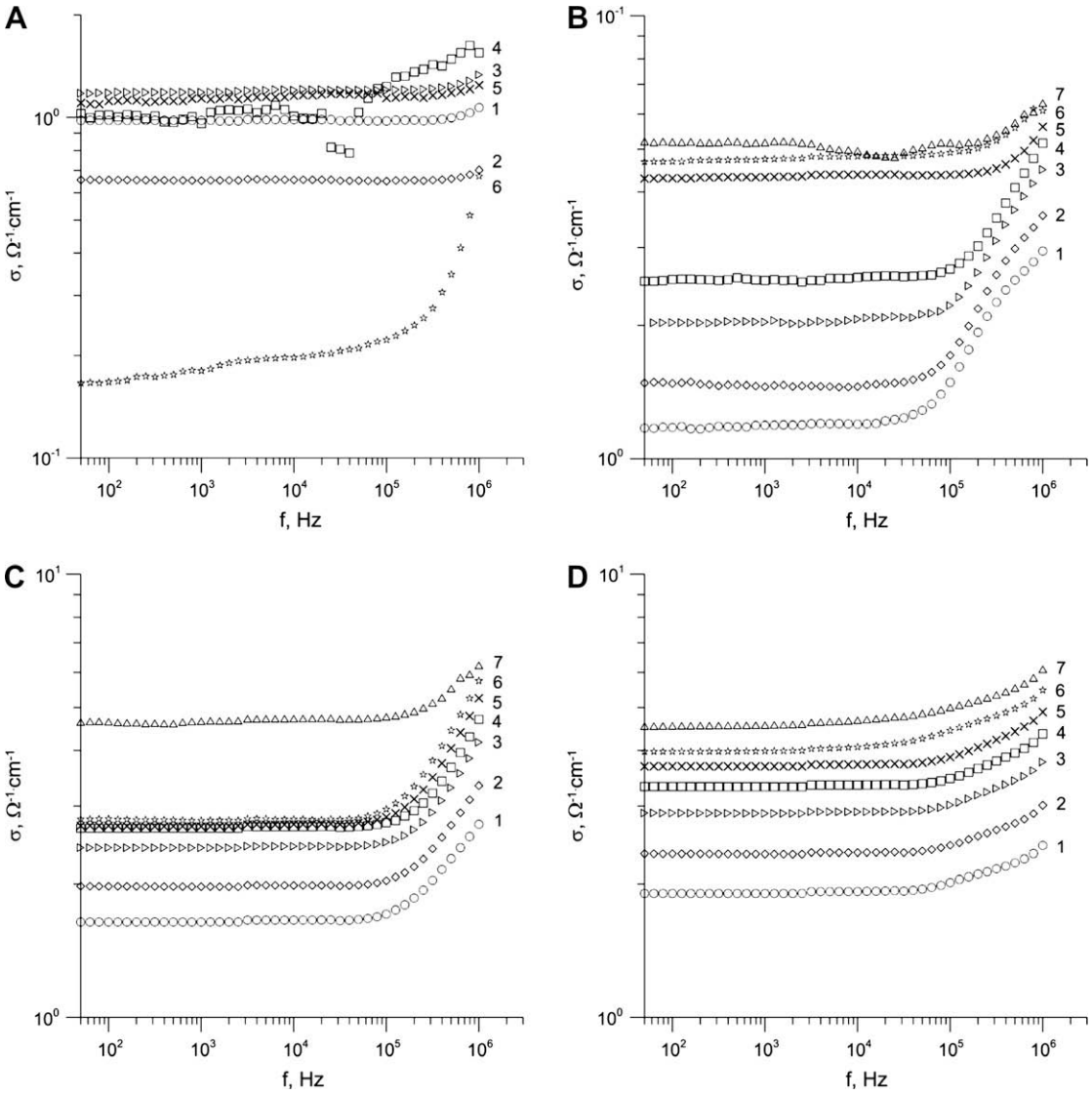

Fig. 2. $\sigma_{real}(T, f)$ dependences for the sample with $x \approx 42$ at.% at different isochronous annealing temperatures T_{ann}: A – as-deposited; B – $T_{ann} = 398$ K; C – 548 K; D – 648 K; 1 – $T = 79$ K; 2 – 113 K, 3 – 158 K, 4 – 203 K, 5 – 248 K, 6 – 288 K and 7 – 353 K.

of $\sigma_{real}(f)$ dependences in the annealed samples have sigmoid-like shape which becomes apparent at $150 < T < 290$ K (see, curves 3 and 6 in Fig. 1b). In so doing, the highest drop for the sigmoidal parts of $\sigma_{real}(f)$ is observed after low-temperature annealings at $T_{ann} \sim 398$–423 K and then this drop is narrowed with T_{ann}, however, extending to the lowest temperatures of measurements (down to 79 K in Fig. 1d). After annealings at the highest value of $T_{ann} = 648$ K a simple sigmoidal shape of $\sigma_{real}(f)$ at $T > 250$ K is transformed into the double sigmoidal curve (see, curves 5–7 in Fig. 1d). As a whole, for $x < 40$ at.% the $\sigma_{real}(f)$ dependences are described by the relation which is characteristic of hopping conductance

$$\sigma_{real}(f) \approx \sigma_o f^{\alpha}, \quad (1)$$

where σ_o is the coefficient and the exponent α has maxima in the inflection points of sigmoidal $\sigma_{real}(f)$ curves. In accordance with a model of hopping conduction developed in [8], $\sigma_{real}(f)$ dependences have sigmoidal character due to the dependence of the exponent α in (1) on proportion of probability p for the electron to make jump from the ground state in the line of the external electric field and probability $(1 - p)$ for him to return back to the initial state. As was shown in [8], for $p << 1$ $\alpha = 2$ and for $p = 0.5$ $\alpha \approx 0$. So for the intermediate values of p the magnitudes of α are changed between 0 and 2.

Note that actual independence of the positions of curves in Fig. 1 for $T = 79$ K on T_{ann} indicates the lack of structure relaxation (invariability of the localized states density) in dielectric matrix after all stages of annealings studied.

In the initial films with x around the x_C ($\sim 42 \div 49$ at.%) conductivity increases but the $\sigma_{real}(f)$ dependences practically stop to depend on frequency (excluding the highest T) and show $\sigma_{real}(T)$ mixed between the samples with $x < 40$ at.% and $x > 49$ at.% (Fig. 2a). This means the presence of competition between the activational (giving $(d\sigma/dT) > 0$) and the metallic (giving $(d\sigma/dT) < 0$) mechanisms of carrier transport for these samples. After annealing the $\sigma_{real}(T)$ behaviour again corresponds to the activational law with $(d\sigma/dT) > 0$ but without sigmoidal $\sigma_{real}(f)$ (as was observed for $x < 40$ at.%). In so doing, the values of σ_{real} (79 K) are increased a little and α in eq. (1) decreases with T_{ann} for this kind of

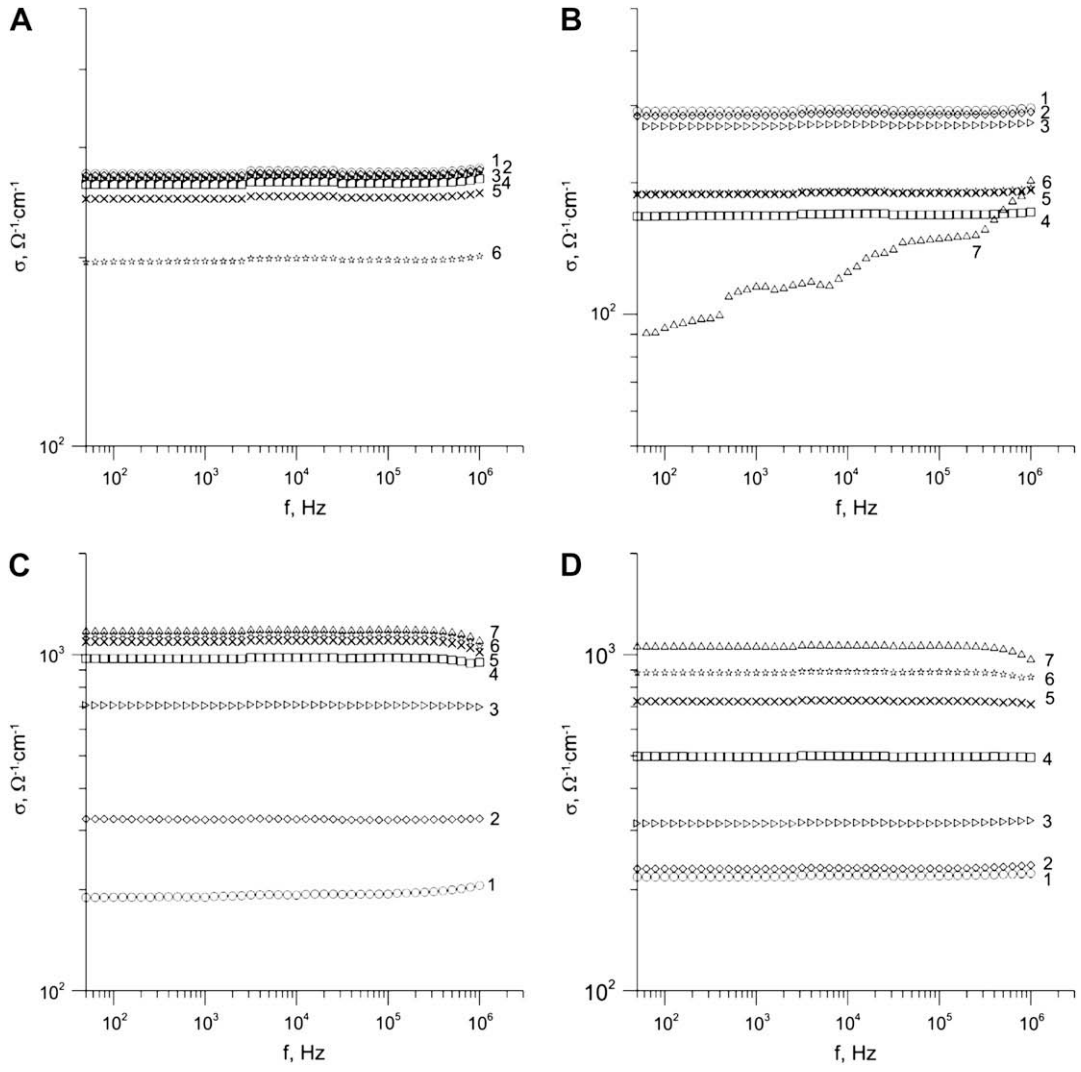

Fig. 3. $\sigma_{real}(T, f)$ dependences for the sample with $x \approx 64$ at.% at different isochronous annealing temperatures T_{ann}: A – as-deposited; B – $T_{ann} = 398$ K; C – 548 K; D – 648 K; 1 – $T = 79$ K; 2 – 113 K, 3 – 158 K, 4 – 203 K, 5 – 248 K, 6 – 288 K and 7 – 353 K.

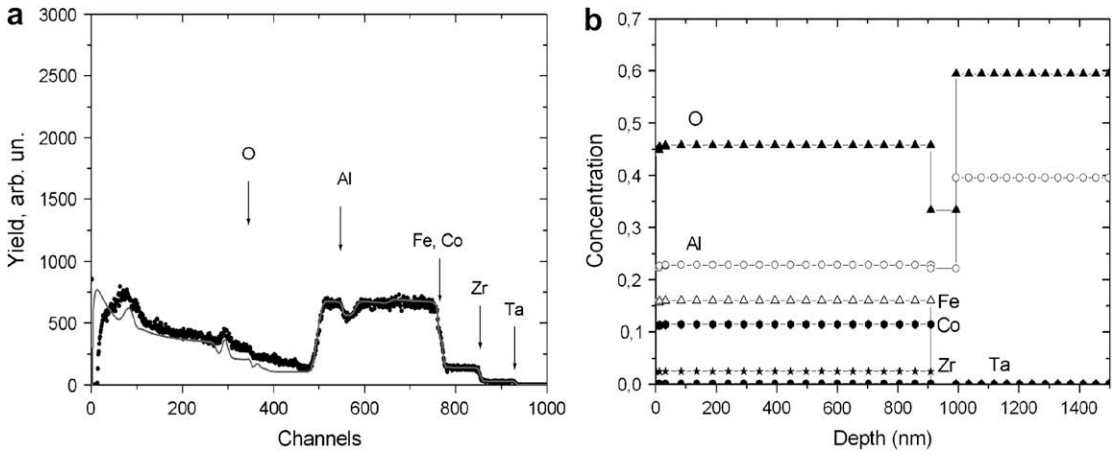

Fig. 4. BS spectra (a) and depth distributions (b) of elements in the sample with $x < x_C$.

samples that shows the change of hopping conditions in dielectric matrix (probably due to the influence of tunneling contribution as observed in [3] after continuous (not step-like) annealing of the samples with $x < 40$ at.%).

As can be seen in Fig. 3*a*, at $49 < x \leq 64$ at.% progress of $\sigma_{real}(T)$ in the as-deposited films corresponds to the power-like law with $(d\sigma/dT) < 0$ that correlates with metallic behaviour observed for DC conductance in these samples [3,5,6]. Moreover, the initial films beyond the x_C display strong increase of σ_{real} with x (as compared with that in the samples with $x \approx x_C$) and vanishing of its dependence on frequency. However, after the annealing procedure progress of $\sigma_{real}(T)$ begin drastically to depend on T_{ann}. For example, in the annealed at $T_{ann} \leq 498$ K the samples with $x \approx 53$ at.% shape of $\sigma_{real}(T)$ is not dependent on T_{ann} whereas at $T_{ann} \geq 498$ K progress of $\sigma_{real}(T)$ is drastically transformed changing the sign of $(d\sigma/dT)$ from positive at low temperatures to $(d\sigma/dT) < 0$ at high temperatures. For the films with x values around 64 at.% after annealings at $T_{ann} \geq 498$ K the sign of $(d\sigma/dT)$ becomes positive at all temperatures of measurements (see, Fig. 3c,d) that probably indicates recovery of non-metallic behaviour of annealed samples.

The reasons for this change of $(d\sigma/dT)$ sign in the nanocomposites with the initially metallic behaviour require additional study of structural transformations in the composites after annealings. But in any case, in our opinion, there are two possible reasons for this transformation of the carrier transport mechanisms in the samples far beyond of the percolation threshold under subjection of the step-like isochronous annealing procedure: (i) recrystallization of metallic phase as was observed in [3]; (ii) break-down of the continuous percolative net consisting of metallic nanoparticles.

Taking into account that recrystallization of metallic percolative net observed in [3] after continuous (not step-like) annealing at much higher temperatures (starting with 750 K for the samples beyond the x_C) than maximal $T_{ann} \approx 647$ K in our experiments, we can suggest predominance of the reason (ii). We can associate the above mentioned recovery of the dielectric state in the initially metallic samples with the oxidation of metallic nanoparticles, forming percolative net, by oxygen atoms randomly distributed by the as-deposited nanocomposites. The possibility of oxidation is confirmed by an excess of oxygen content in the studied samples over its stoichiometric value in alumina estimated from the Backscattering Spectrometry results shown in Fig. 4[1]. As can be seen, the observed ratio O/Al $\approx 0.45/0.23 \approx 2$ exceeds the stoichiometric 1.5 for Al_2O_3).

4. Conclusion

The studied nanocomposites reveal strong variations of AC electrical conductivity with temperature and frequency after step-like isochronous (15 min) annealings within the temperature range from 398 K to 648 K. The observed $\sigma_{real}(T, f)$ dependences in the as-deposited films display transition from dielectric to metallic behaviour when crossing the percolation threshold x_C. After annealing of the samples below the x_C the $\sigma_{real}(T, f)$ progress follows the hopping law with the sigmoidal frequency dependence. The samples being far beyond the percolation threshold revealed transition from metallic to activational $\sigma_{real}(T)$ law after high-temperature annealing attributed to the internal oxidation of metallic nanoparticle by excess of oxygen presented in the as-deposited samples.

Acknowledgement

The authors would like to acknowledge the financial support from VISBY Program of the Swedish Institute.

References

[1] Stauffer D, Aharony A. Introduction to percolation theory. London: Taylor and Francis; 1992.
[2] Salz D, Wark M, Baalmann A, Simon U, Jaeger N. Phys Chem Chem Phys 2002;4:2438–42.
[3] Yu Kalinin, Remizov A, Sitnikov A. Solid State Physics 2004;4:2076–82.
[4] Fedotova J, Kalinin Yu, Fedotov A, Sitnikov A, Svito I, Zalesskij A, et al. Hyperfine Interaction 2005;165:127–34.
[5] Saad AM, Fedotov AK, Fedotova JA, Svito IA, Andrievsky BV, Kalinin YuE, et al. Phys Stat Sol (c) 2006;3:1283–90.
[6] Saad AM, Fedotov AK, Svito IA, Mazanik AV, Andrievski BV, Patryn AA, et al. Progr in Solid State Chem 2006;14:139–46.
[7] Żukowski P, Kołtunowicz T, Partyka J, Węgierek P, Fedotova JA, Fedotov AK, et al. Electrical Review 2008;84(3):244–6.
[8] Żukowski P, Kołtunowicz T, Partyka J, Węgierek P, Kolasik M, Larkin AV, et al. Electrical Review 2008;84(3):247–9.

[1] Authors thank very much Dr. E. Szilagyi from KFKI Research Institute for Particle and Nuclear Physics (Budapest, Hungary) for BS data.